Effect of Processing Variables on the Morphology of Electrospun Poly[(lactic acid)-*co*-(glycolic acid)] Nanofibers

Fujuan Liu, Rui Guo, Mingwu Shen, Shanyuan Wang, Xiangyang Shi*

A systematic study of the effects of $\overline{M}_w$, flow rate, voltage, and composition on the morphology of electrospun PLGA nanofibers is reported. It is shown that changes of voltage and flow rate do not appreciably affect the morphology. However, the $\overline{M}_w$ of PLGA predominantly determines the formation of bead structures. Uniform electrospun PLGA nanofibers with controllable diameters can be formed through optimization. Further, multi-walled carbon nanotubes can be incorporated into the PLGA nanofibers, significantly enhancing their tensile strength and elasticity without compromising the uniform morphology. The variable size, porosity, and composition of the nanofibers are essential for their applications in regenerative medicine.

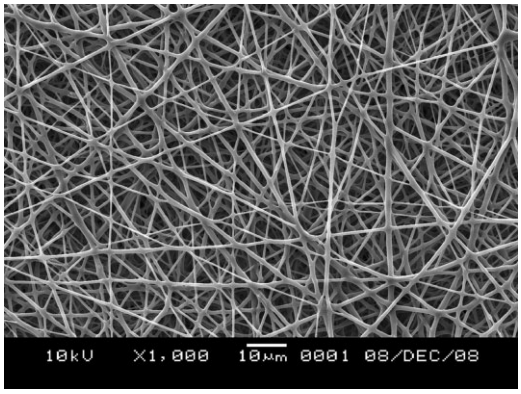

Introduction

Electrospinning is an efficient method for forming fibers with sub-μm diameters through the action of electrostatic forces. This technique has been introduced by Formhals[1] in 1934. Since then, there have been a few exploratory studies on polymer electrospinning.[2] In the past decades, interest in electrospinning process has been greatly arisen due to the fact that the diameter of electrospun polymer fibers is able to be reduced to a range of a nanometer to a few micrometers.[3–10] Electrospun mats composed of nanofibers have a large specific surface area and very small pore size when compared to commercial mats. Therefore, it was used in a variety of applications such as filter membranes, protective clothing, fiber reinforcement in composite materials, tissue engineering scaffolds, and drug delivery systems.[11–24] To date, many synthetic or naturally occurring polymers have been electrospun to form fibers. The research is primarily focused on the structure, morphology, and transport and permeability properties of electrospun nanofibers.[4,12,25,26]

As a biocompatible and biodegradable polymer, poly[(lactic acid)-*co*-(glycolic acid)] (PLGA) has been fabricated to form three-dimensional scaffolds using different micro- and nano-fabrication techniques,[27–30] such as gas foaming,[29] microsphere sintering,[30] and electrospinning.[31–35] Electrospun nanofibrous PLGA mats have good performance; it is thus considered as an important biomedical material in the general area of regenerative medicine, such as controlled drug/protein delivery systems and as scaffolds for tissue engineering. During the process of electrospinning, a number of parameters can greatly influence the properties of the generated fibers.[26,36] These

F. Liu, R. Guo, M. Shen, S. Wang, X. Shi
Key Laboratory of Textile Science and Technology, Ministry of Education, Donghua University, Shanghai 201620, China
F. Liu, S. Wang
College of Textiles
Donghua University, Shanghai 201620, China
R. Guo, M. Shen, X. Shi
College of Chemistry, Chemical Engineering, and Biotechnology, Donghua University, Shanghai 201620, China
E-mail: xshi@dhu.edu.cn

Macromol. Mater. Eng. **2009**, *294*, 666–672

DOI: 10.1002/mame.200900110

variables include $\overline{M}_w$ (intrinsic viscosity), applied voltage, flow rate, solution concentration, tip-to-collector distance, and composition, etc. Previous investigations show that polymer concentration and the tip-to-collector distance are closely associated with the diameter of the electrospun fibers.[26] However, there are few reports related to a systematic study on the effect of molecular weight, flow rate, applied voltage, and composition on the morphology of the electrospun PLGA nanofibers.

In this present study, electrospun PLGA nanofibers were fabricated under various processing parameters. The systematic change of the processing variables is important for us to optimize the fiber formation condition and to obtain the tailor-made fiber mats. Uniform PLGA nanofibers with a variable diameter, porosity, and morphology were formed under the optimized conditions. Additionally, we show that multi-walled carbon nanotubes (MWNTs) could be incorporated into PLGA nanofibers under the optimal electrospinning conditions. The electrospun composite nanofibrous mat is expected to have superior mechanical properties when compared to the pure PLGA nanofibers. These PLGA or PLGA/MWNT composite nanofibers were completely characterized using scanning electron microscopy (SEM), attenuated total reflection Fourier-transform infrared (ATR-FTIR) spectroscopy, DSC, and porosity. The formed PLGA nanofibers should be readily useful for future development of tissue engineering scaffold materials.

Experimental Part

Materials

PLGA ($\overline{M}_w = 15\,000$, 45 000, and 81 000 $g \cdot mol^{-1}$) was purchased from Jinan Daigang Biomaterial Co., Ltd. (China). PLGA with $\overline{M}_w = 28\,000$ and 57 000 $g \cdot mol^{-1}$ was from Sigma-Aldrich. Tetrahydrofuran (THF) and *N,N*-dimethylformamide (DMF) were from Sinopharm Chemical Reagent Co., Ltd. (China). MWNTs (diameter = 30–70 nm, length = 100–400 nm) with carboxyl residues (MWNT-COOH) were obtained according to previous reports.[37–39]

Electrospinning

The PLGA with various molecular weights were dissolved in a mixture of THF/DMF (v/v = 3:1) at a concentration of 10% ($g \cdot mL^{-1}$) before the electrospinning process. The experimental set-up consisted of a 10 mL syringe, a stainless steel needle with an inner diameter of 1.0 mm, a high voltage power supplier (Institute of Beijing High Voltage Technology, Beijing, China) and a collector which was positioned vertically (Figure 1). A clamp was used to connect the high voltage power supplier (positive voltage ranging from 0 to 40 kV) with the needle. The collector was covered with aluminum foil with a tip-to-collector distance of about 150 mm and was grounded directly. The polymer jets emerged from the Taylor Cone under the high electrical field forming the ultra-fine fibers, which were collected on the aluminum foil. Subsequently, the aluminum foil was removed from the collector, and the samples were air dried for at least 24 h before characterization. The electrospinning experiments were performed at room temperature.

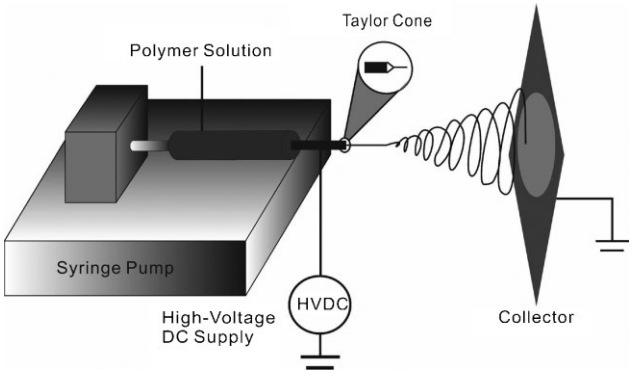

Figure 1. Setup of the electrospinning system.

SEM

SEM was performed using a JEOL JSM-5600LV electron microscope with an accelerating voltage of 10 kV. The nanofiber samples were sputter coated with a 10 nm thick gold film before measurements. The fiber diameters were determined using Image J software (developed by the U.S. National Institutes of Health). At least 100 nanofibers in different SEM images were analyzed for each sample.

ATR-FTIR Spectroscopy

ATR-FTIR was carried out using a Nicolet Nexus670 FT-IR spectrometer. All spectra were recorded in a wavenumber range of 4 000–500 cm^{-1}. The raw PLGA was dissolved in a mixture of THF/DMF (v/v = 3:1). The dispersion was casted on a silicon wafer and air-dried. Two electrospun PLGA mats ($\overline{M}_w = 81\,000\ g \cdot mol^{-1}$) with an excellent morphology were selected for ATR-FTIR measurements.

Differential Scanning Calorimetry

DSC was performed using a DSC204 F1 calorimeter. The samples were heated at 5 °C · min^{-1} in a nitrogen atmosphere with a temperature control range from 0 to 100 °C. The values of the glass transition temperature (T_g) were obtained from the dynamic thermograms.

Porosity of Nanofibrous Mats

The thickness of the electrospun mats was measured with a micrometer. The apparent density (ρ_a) and porosity (ε) were obtained from the following equations:[40]

$$\rho_a = \frac{m}{\pi r^2 h} \quad (1)$$

$$\varepsilon = \left(1 - \frac{\rho_a}{\rho_b}\right) \times 100\% \quad (2)$$

where m, r, and h are mass, radius, and thickness of the electrospun nanofibrous mat. Bulk density (ρ_b) of PLGA was $1.25\ g \cdot cm^{-3}$.

Mechanical Measurements

The mechanical properties of electrospun fibrous mats were conducted by a materials testing machine (H5K-S, Hounsfield, UK) at 20 °C, relative humidity of 63%, and an elongation speed of $10\ mm \cdot min^{-1}$. First, the electrospun mats were punched into small strips with width × gauge length = $10 \times 50\ mm^2$, and five strips from different sites of each fibrous sample were chosen for the tensile test. Then the stress/strain curves were obtained from the load deformation curves recorded. Both PLGA and PLGA/MWNT mats were tested.

Results and Discussion

Morphologies of Electrospun Nanofibrous Mats

The fiber jet stability is closely associated with the applied voltage during the electrospinning process. When the voltage was lower than 14 kV, we found that polymer droplets dropped down continuously from the tip of the needle. However, when the voltage was increased to 23 kV, the jet started to become quite unstable, resulting in two fiber jets at the tip of the needle occasionally. Therefore, the voltage range of 14–22 kV was selected for subsequent studies.

Figure 2 exhibits SEM micrographs of electrospun PLGA nanofibers ($\overline{M}_w = 57\,000\ g \cdot mol^{-1}$) under different voltages (from 14 to 22 kV). It is clear that the voltage change did not appreciably affect the morphology of the PLGA fibers. The smooth fibers were obtained in all cases. Additionally, the fiber diameter was found to be 412, 553, 524, 751, and 636 nm at the voltage of 14, 15, 18, 20, and 22 kV, respectively (Table 1). The diameter of the fibers increases non-linearly with the voltage, which is consistent with results reported in literature.[41] The diameter distribution histograms of the nanofibers formed under various applied voltages (Figure 2) show that the formed PLGA fibers are relatively uniform. Since the optimized voltage range is in between 14–22 kV, we selected 20 kV for the subsequent experiments.

Figure 3 shows the SEM images of electrospun PLGA nanofibers with various $\overline{M}_w$s under fixed conditions (applied voltage: 20 kV, flow rate: $1\ mL \cdot h^{-1}$). Bead structure was formed for PLGA with lower $\overline{M}_w$ ($15\,000\ g \cdot mol^{-1}$) [Figure 3(a)], which may be ascribed to the lower intrinsic viscosity of the polymers. When the $\overline{M}_w$ was increased to $28\,000\ g \cdot mol^{-1}$, bead structure along with some extra-fine

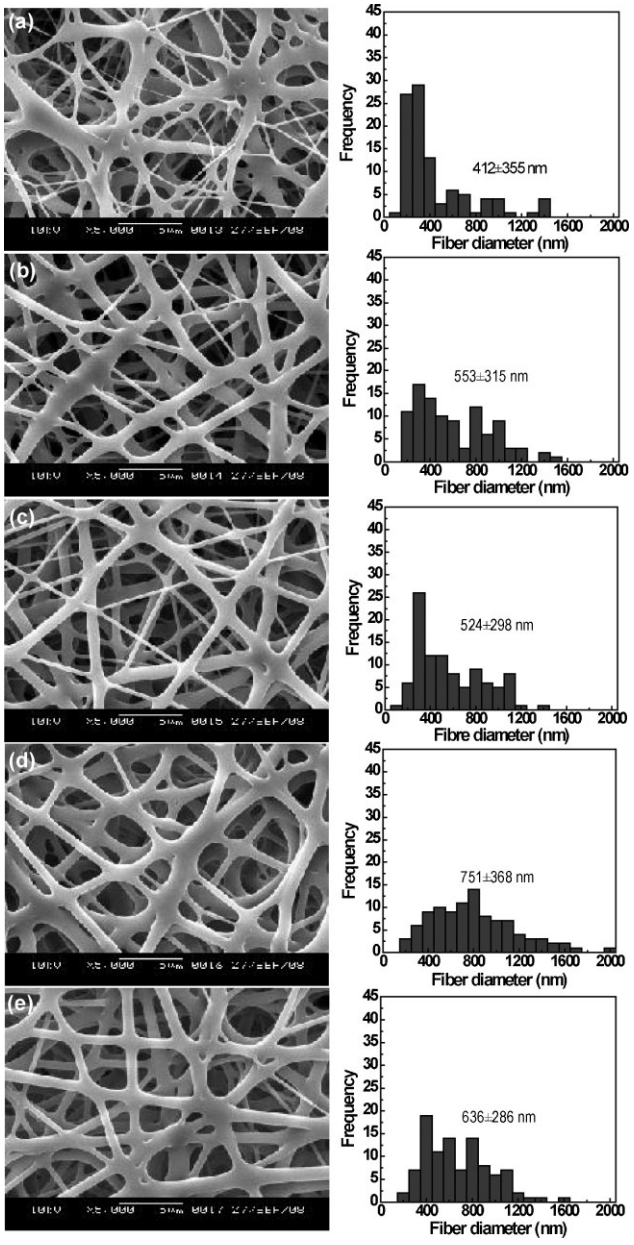

Figure 2. SEM micrographs and the diameter distribution histograms of the PLGA ($\overline{M}_w = 57\,000\ g \cdot mol^{-1}$) nanofibers under the voltage of (a) 14, (b) 15, (c) 18, (d) 20, and (e) 22 kV (flow rate: $1\ mL \cdot h^{-1}$). The diameter distribution histogram data are representative of independent experiments and all data are given as means ± SD ($n = 100$).

fibers was formed [Figure 3(b)]. Further increasing the $\overline{M}_w$ of PLGA ($45\,000\ g \cdot mol^{-1}$) resulted in smaller and spindle-like bead structure [Figure 3(c)]. In addition, the fibers between the beads have a circular cross-section, with a typical diameter of 142 nm. Uniform fibrous structures were formed when the $\overline{M}_w$ was $57\,000\ g \cdot mol^{-1}$ or more [Figure 2(d) and 3(d)]. The fibers still exhibit a circular cross-section with a diameter of 751 nm [Figure 2(d)]. For

Macromol. Mater. Eng. **2009**, *294*, 666–672

Macromolecular Journals

DOI: 10.1002/mame.200900110

Table 1. Characteristics of electrospun nanofibrous PLGA ($\overline{M}_w = 57\,000\ g \cdot mol^{-1}$) mats under different applied voltages. The flow rate was kept at $1\ mL \cdot h^{-1}$.

Applied voltage	Fiber diameter	Apparent density	Porosity
kV	nm	$g \cdot cm^{-3}$	%
14	412 ± 355	0.40 ± 0.06	68 ± 5
15	553 ± 315	0.60 ± 0.11	52 ± 9
18	524 ± 298	0.43 ± 0.03	59 ± 7
20	751 ± 368	0.39 ± 0.13	53 ± 6
22	636 ± 286	0.45 ± 0.09	64 ± 7

PLGA with $\overline{M}_w$ of $81\,000\ g \cdot mol^{-1}$, excellent fiber morphology with a diameter of 499 nm was obtained [Figure 3(d)]. The diameter distribution histogram of the PLGA nanofibers [Figure 3(e)] shows that the fibers have a relatively uniform morphology.

Flow rate is an important parameter to control the fiber morphology. When $\overline{M}_w$ was kept at $81\,000\ g \cdot mol^{-1}$, a flow rate of $1\ mL \cdot h^{-1}$ gave rise to an excellent morphology of PLGA fibers [Figure 3(d) and (e)]. The morphology of fibers formed at other flow rates (0.5 and $2\ mL \cdot h^{-1}$) was also investigated (Figure 4). At the flow rate of $2\ mL \cdot h^{-1}$ [Figure 4(d) and 4(e)], non-uniform distribution of the PLGA nanofibers with an average diameter of 586 nm [Figure 4(f)] was observed, which is probably due to the instability of the jets. As the flow rate was decreased (1 and $0.5\ mL \cdot h^{-1}$), the fiber diameter distribution becomes homogeneous [Figure 3(d) and (e)] for $1\ mL \cdot h^{-1}$ flow rate, Figure 4(a)–(c) for $0.5\ mL \cdot h^{-1}$ flow rate). Furthermore, the fiber diameter decreased with decrease in the flow rate (499 nm at $1\ mL \cdot h^{-1}$ flow rate, and 465 nm at $0.5\ mL \cdot h^{-1}$ flow rate). These results are consistent with literature data.[42]

ATR-FTIR

The electrospun PLGA nanofiber mats were characterized using ATR-FTIR (curves b and c in Figure 5). The peaks at $1\,754\ cm^{-1}$ (C=O stretching vibration from ester bonds), two peaks at 1 423 and $1\,391\ cm^{-1}$ (wagging vibrations from saturated C–H bonds), and two peaks at 1 167 and $1\,090\ cm^{-1}$ (C–O stretching vibration from ether groups[43]) are characteristic features of PLGA polymer, regardless of whether it is a raw material or in a fiber form. The peak at $1\,672\ cm^{-1}$ of raw PLGA may be caused by C=O stretching vibration from amide bands of the residual solvent DMF (Curve a in Figure 5).[44] Compared to the electrospun PLGA nanofibers with higher surface-to-volume ratio, it is more difficult for the raw PLGA film formed through solution casting to evaporate the DMF solvent. This further suggests that the formed PLGA nanofibers can be easily purified from organic solvent, thereby significantly improving the biocompatibility and biosafety of the materials for biomedical applications.

DSC

The thermal properties of electrospun PLGA mats were examined using DSC (Figure 6). It is clear that PLGA has an amorphous behavior, with a glass transition temperature

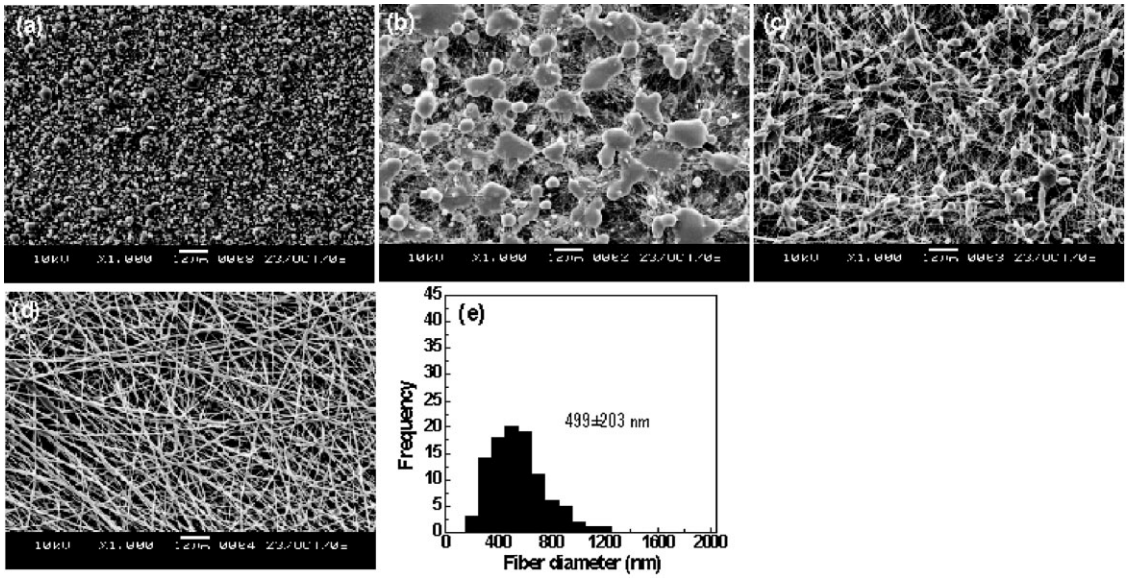

Figure 3. SEM micrographs of electrospun PLGA nanofibers with $\overline{M}_w$s of (a) 15 000, (b) 28 000, (c) 45 000, (d) $81\,000\ g \cdot mol^{-1}$ (applied voltage: 20 kV, flow rate: $1\ mL \cdot h^{-1}$). (e) Shows the diameter distribution histogram of the PLGA nanofibers shown in (d).

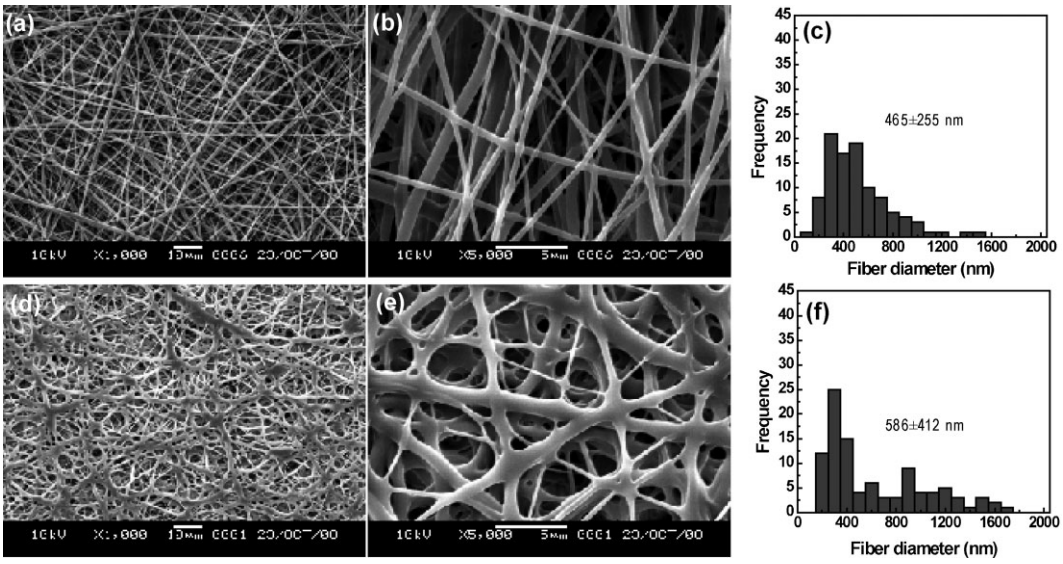

Figure 4. SEM micrographs of electrospun PLGA nanofibers with $\overline{M}_w = 81\,000\ g \cdot mol^{-1}$ at the flow rates of (a, b) 0.5 and (d, e) $2\ mL \cdot h^{-1}$, respectively. (b) and (e) are high-magnification images of (a) and (d), respectively. (c) and (f) show the diameter distribution histogram of the PLGA nanofibers shown in (a) and (d), respectively.

(T_g) of around 50 °C for all the samples. The T_g of the electrospun mats (curves b and c in Figure 6) is lower than that of the raw PLGA (curve a in Figure 6). This could be due to the improvement in the orientation of molecular chains in the electrospun polymer nanofibers[45,46] as well as the larger area to volume ratio of electrospun fibers.[10,46] In addition, the crystallinity of the fiber structure is expected to decrease appreciably when compared to the raw PLGA materials. In other words, the chain entanglement in bulk form is much higher when compared to the same polymer in nanofiber form.[10] This result is in agreement with literature data.[10,45,46]

Porosity

Porosity is an important parameter for nanofiber materials used for tissue engineering scaffolds. A perfect 3-dimensional nanofibrous scaffold can afford not only cell attachment, proliferation, and differentiation, but also sufficient transport for nutrients and waste removal. Apparent density and porosity of electrospun PLGA mats were calculated using Equation (1) and (2), and are summarized in Table 2. As the fiber diameter increases, porosity of electrospun mat generally decreases, due to numerous fiber junctions caused by higher flow rate

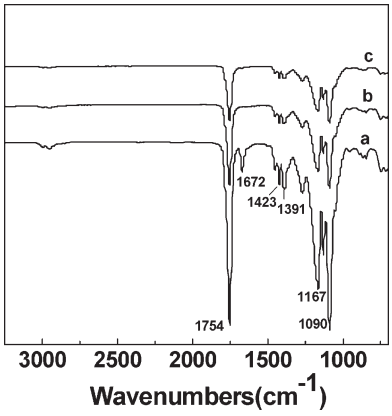

Figure 5. ATR-FT-IR spectra of (a) raw PLGA and (b, c) electrospun PLGA nanofibrous mats ($\overline{M}_w = 81\,000\ g \cdot mol^{-1}$) formed at a voltage of 20 kV and flow rates of (b) $1\ mL \cdot h^{-1}$ and (c) $0.5\ mL \cdot h^{-1}$.

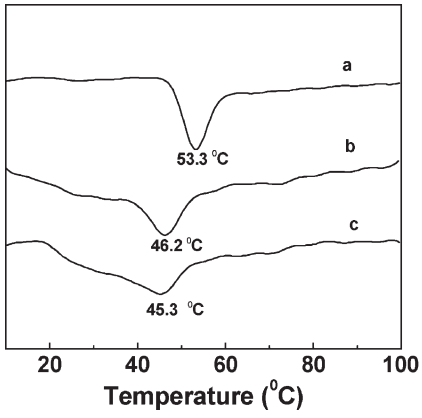

Figure 6. DSC profiles of (a) raw PLGA, and (b, c) electrospun PLGA nanofibers ($\overline{M}_w = 81\,000\ g \cdot mol^{-1}$) formed at a voltage of 20 kV and at the flow rates of (b) $1\ mL \cdot h^{-1}$ and (c) $0.5\ mL \cdot h^{-1}$.

Macromolecular Journals
DOI: 10.1002/mame.200900110

Table 2. Apparent density and porosity of the two typical electrospun PLGA nanofibrous mats. Data are representative of independent experiments and all data are given as mean ± SD ($n = 3$).

Sample	Fiber diameter	Apparent density	Porosity
	nm	$g \cdot cm^{-3}$	%
mat 1[a)]	499 ± 203	0.45 ± 0.04	64 ± 3
mat 2[b)]	465 ± 255	0.36 ± 0.08	71 ± 7

[a)] $\overline{M}_w = 81\,000\ g \cdot mol^{-1}$, applied voltage: 20 kV, flow rate: $1\ mL \cdot h^{-1}$; [b)] Flow rate: $0.5\ mL \cdot h^{-1}$, other processing parameters are the same as for mat 1.

($1\ mL \cdot h^{-1}$) [Figure 3(d)]. When flow rate was kept at $0.5\ mL \cdot h^{-1}$, porosity of electrospun PLGA mat can reach 71%.

Mechanical Measurements

As the 3-D scaffolds for cell culture purposes are expected to be robust enough to support attachment, proliferation, and differentiation of cells, mechanical properties of the scaffolds are quite vital in tissue engineering. It is known that carbon nanotubes are one of the most promising nanofibers that mimic the extracellular matrix.[47] Zhao et al.[48] have shown the potential of carbon nanotubes to mimic the role of collagen and serve as scaffolds for the growth of hydroxyapatite. Apart from nanoscale features, carbon nanotubes possess unique physical, chemical, and mechanical properties that distinguish them from other nanofibrous materials used for tissue engineering applications. We expect that electrospun PLGA/carbon nanotube composite nanofibers should display excellent mechanical properties.

In this study, we mixed MWNTs with PLGA ($\overline{M}_w = 81\,000\ g \cdot mol^{-1}$) with a mass ratio of (1:100) before the electrospinning process. The formed composite PLGA/MWNT nanofibers [Figure 7(a)] display similar morphology to that of pure PLGA nanofibers [Figure 3(d)]. The diameter of the PLGA/MWNT nanofibers did not show any significant changes when compared to the pure PLGA nanofibers [Figure 7(b) and 3(e)]. However, the mechanical property of the PLGA/MWNTs nanofibers were significantly enhanced even with only 1.0 wt.-% MWNTs mixed with PLGA (Table 3). Figure 7(c) shows the typical stress/strain curves of electrospun PLGA nanofibers with and without MWNTs. It is observed that tensile stress (5.23 MPa) and the ultimate strain (128.77%) of electrospun PLGA/MWNT fibrous mat are significantly higher than those of pure PLGA nanofibers (tensile stress was 3.50 MPa, and ultimate strain was 58.64%). In addition, the composite PLGA/MWNT nanofibers exhibit a much higher Young's modulus (188 ± 14 MPa) when compared to that of pure PLGA nanofibers (100 ± 10 MPa). The enhanced mechanical properties of the composite PLGA/MWNT nanofiber mats should be ascribed to the presence of MWNTs uniformly dispersed in the PLGA matrix. Furthermore, most of the MWNTs in the fiber structures orientated parallel to the axis of electrospun PLGA nanofibers;[49] therefore, the load can be transferred efficiently from the PLGA matrix to the nanotubes. Finally, the porosity of the electrospun PLGA/MWNT nanofibers (76%) is higher than that of the PLGA nanofibers (71%) (Table 2), presumably due to the hollow interior nature of the MWNTs.

Table 3. Mechanical properties of electrospun PLGA and PLGA/MWNT nanofibers under the same operating conditions: $\overline{M}_w$ of PLGA = $81\,000\ g \cdot mol^{-1}$, applied voltage = 20 kV, flow rate = $1\ mL \cdot h^{-1}$. Data are representative of independent experiments and all data are given as mean ± SD ($n = 5$).

Sample	Tensile stress	Ultimate strain
	MPa	%
PLGA	3.50 ± 1.32	58.64 ± 35.45
PLGA/MWNTs	5.23 ± 1.36	128.77 ± 40.81

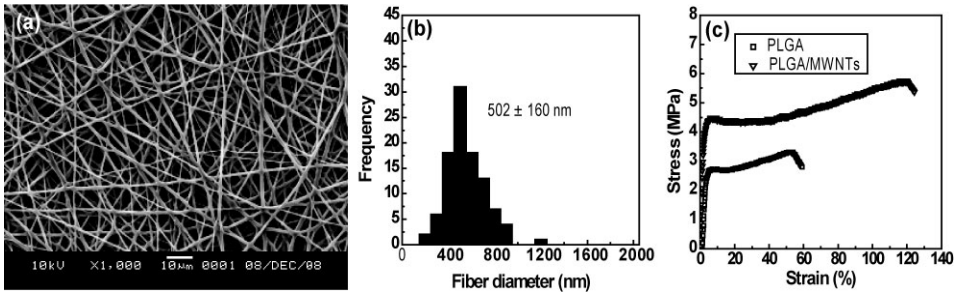

Figure 7. (a) SEM micrograph and (b) diameter distribution histogram of PLGA/MWNT composite nanofibers formed at a voltage of 20 kV and at the flow rate of $1\ mL \cdot h^{-1}$. (c) Stress/strain curves for electrospun PLGA and PLGA/MWNT nanofibers, respectively. The PLGA with $\overline{M}_w = 81\,000\ g \cdot mol^{-1}$ was used.

Conclusion

The effect of molecular weight, flow rate, voltage, and composition on the morphology and properties of the electrospun PLGA nanofibers was systematically studied. At a certain constant electrospinning condition, the molecular weight ($\overline{M}_w$) of PLGA and flow rate predominantly determines the formation of bead structure on nonwoven mats. Through a judicious selection and optimization, electrospun PLGA nanofibrous mats with excellent morphology can be formed. The electrospun mats show good porosity superior to those of the casting film mainly as a result of the enlarged surface area. In addition, under the optimized conditions, electrospun PLGA/MWNT composite mats with relative uniform diameter distribution can be fabricated. The formed PLGA/MWNT composite mats noticeably exhibit superior mechanical properties and porosity to those of pure PLGA mats. The electrospun PLGA and PLGA/MWNT composite nanofibers could be used for the future development of tissue engineering scaffold materials, which is currently going on in our laboratory.

Acknowledgements: This study was jointly supported by the *Programme of Introducing Talents of Discipline to Universities*, B07024 and *Young Teacher Foundation of Donghua University*, no. 200802. X. S. acknowledges support from the *Program for Professor of Special Appointment (Eastern Scholar)* at *Shanghai Institutions of Higher Learning*. Dr. *Elijah J. Petersen* at the University of Michigan is thanked for providing the multi-walled carbon nanotubes.

Received: April 23, 2009; Revised: June 22, 2009; Published online: August 14, 2009; DOI: 10.1002/mame.200900110

Keywords: carbon nanotubes; electrospinning; morphology; nanofibers; poly[(lactic acid)-*co*-(glycolic acid)]

[1] US 1975504 (1934), inv.: A. Formhals.
[2] L. Larrondo, R. St., John Manley, *J. Polym. Sci.* **1981**, *19*, 909.
[3] J. M. Deitzel, W. Kosik, S. H. McKnight, N. C. Beck Tan, J. M. DeSimone, S. Crette, *Polymer* **2002**, *43*, 1025.
[4] Y. M. Shin, M. M. Hohman, M. P. Brenner, G. C. Rutledge, *Polymer* **2001**, *42*, 09955.
[5] D. H. Reneker, A. L. Yarin, E. Zussman, H. Xu, in: *Advances in Applied Mechanics*, Vol. 41, H. Aref, E. van der Giessen, Eds., Elsevier, Amsterdam 2007, p. 43.
[6] S. A. Theron, E. Zussman, A. L. Yarin, *Polymer* **2004**, *45*, 2017.
[7] D. H. Reneker, A. L. Yarin, *Polymer* **2008**, *49*, 2387.
[8] J. Du, Y. L. Hsieh, *Nanotechnology* **2008**, *19*, 125707/1.
[9] H. Liu, Y. L. Hsieh, *J. Polym. Sci., Part: B-Polym. Phys.* **2002**, *40*, 2119.
[10] X. Zong, K. Kim, D. Fang, S. Ran, B. S. Hsiao, B. Chu, *Polymer* **2002**, *43*, 4403.
[11] P. Gibson, H. Schreuder-Gibson, D. Rivin, *Colloid Surf. A Physicochem. Eng. Asp.* **2001**, *187*, 469.
[12] J. Doshi, D. H. Reneker, *J. Electrost.* **1995**, *35*, 151.
[13] R. A. Jonas, G. Ziemer, F. J. Schoen, L. Britton, A. R. Castaneda, *J. Vasc. Surg.* **1988**, *7*, 414.
[14] Y. Marois, N. L. Chakfe, X. Deng, M. Marois, T. How, M. W. King, R. Guidoin, *Biomaterials* **1995**, *16*, 1131.
[15] X. Shi, F. Caruso, *Langmuir* **2001**, *17*, 2036.
[16] M. Goldberg, R. Langer, X. Jia, *J. Biomater. Sci. Polymer Ed.* **2007**, *18*, 241.
[17] K. Ulubayram, A. N. Cakar, P. Korkusuz, C. Ertan, N. Hasirci, *Biomaterials* **2001**, *22*, 1345.
[18] D. A. Grande, *J. Biomed. Mater. Res.* **1997**, *23*, 211.
[19] Z. Ma, M. Kotaki, R. Inai, S. Ramakrishna, *Tissue Eng.* **2005**, *11*, 101.
[20] R. Murugan, S. Ramakrishna, *Tissue Eng.* **2006**, *12*, 435.
[21] X. Zong, H. Bien, C. Y. Chung, L. Yin, D. Fang, B. S. Hsiao, B. Chu, E. Entcheva, *Biomaterials* **2005**, *26*, 5330.
[22] J. A. Lee, K. C. Krogman, M. Ma, R. M. Hill, P. T. Hammond, G. C. Rutledge, *Adv. Mater.* **2009**, *21*, 1252.
[23] M. Roso, S. Sundarrajan, D. Pliszka, S. Ramakrishna, M. Modesti, *Nanotechnology* **2008**, *19*, 285707/1.
[24] S. Sundarrajan, S. Ramakrishna, *J. Mater. Sci.* **2007**, *42*, 8400.
[25] H. Fong, I. Chun, D. H. Reneker, *Polymer* **1999**, *40*, 4585.
[26] A. Koski, K. Yim, S. Shivkumar, *Mater. Lett.* **2004**, *58*, 493.
[27] Y. Lu, S. C. Chen, *Adv. Drug Deliv. Rev.* **2004**, *56*, 1621.
[28] T. K. Kim, J. J. Yoon, D. S. Lee, T. G. Park, *Biomaterials* **2006**, *27*, 152.
[29] M. Borden, M. Attawia, Y. Khan, C. T. Laurencin, *Biomaterials* **2002**, *23*, 551.
[30] D. S. Katti, K. W. Robinson, F. K. Ko, C. T. Laurencin, *J. Biomed. Mater. Res. Part B* **2004**, *70B*, 286.
[31] G. Perale, G. Pertici, C. Giordano, F. Daniele, M. Masi, S. Maccagnan, *J. Appl. Polym. Sci.* **2008**, *108*, 1591.
[32] B. Duan, X. Yuan, Y. Zhu, Y. Zhang, X. Li, Y. Zhang, K. Yao, *Eur. Polym. J.* **2006**, *42*, 2013.
[33] C. A. Bashur, L. A. Dahlgren, A. S. Goldstein, *Biomaterials* **2006**, *27*, 5681.
[34] I. K. Shim, S. Y. Lee, Y. J. Park, M. C. Lee, S. H. Lee, J. Y. Lee, S. J. Lee, *J. Biomed. Mater. Res. Part A* **2008**, *84A*, 247.
[35] Y. You, B. M. Min, S. J. Lee, T. S. Lee, W. H. Park, *J. Appl. Polym. Sci.* **2005**, *95*, 193.
[36] J. M. Deitzel, J. Kleinmeyer, D. Harris, N. C. Beck Tan, *Polymer* **2001**, *42*, 261.
[37] E. J. Petersen, Q. Huang, W. J. Weber, Jr., *Environ. Health Perspect.* **2008**, *116*, 496.
[38] E. J. Petersen, Q. Huang, W. J. Weber, Jr., *Environ. Sci. Technol.* **2008**, *42*, 3090.
[39] M. Shen, S. H. Wang, X. Shi, X. Chen, Q. Huang, E. J. Petersen, R. A. Pinto, J. R. Baker, Jr., W. J. Weber, Jr., *J. Phys. Chem. C* **2009**, *113*, 3150.
[40] T. G. Kim, T. G. Park, *Biotechnol. Prog.* **2006**, *22*, 1108.
[41] C. Meechaisue, R. Dubin, P. Supaphol, V. P. Hoven, J. Kohn, *J. Biomater. Sci. Polym. Ed.* **2006**, *17*, 1039.
[42] T. J. Sill, H. A. von Recum, *Biomaterials* **2008**, *29*, 1989.
[43] I. Armentano, M. Dottori, D. Puglia, J. M. Kenny, *J. Mater. Sci. Mater. Med.* **2008**, *19*, 2377.
[44] F. Chen, X. Q. Li, X. M. Mo, C. L. He, H. S. Wang, Y. Ikada, *J. Biomater. Sci. Polym. Ed.* **2008**, *19*, 677.
[45] W. Cui, X. Li, X. Zhu, G. Yu, S. Zhou, J. Weng, *Biomacromolecules* **2006**, *7*, 1623.
[46] S. Y. Gu, J. Ren, Q. L. Wu, *Synth. Met.* **2005**, *155*, 157.
[47] I. Firkowska, E. Godehardt, M. Giersig, *Adv. Funct. Mater.* **2008**, *18*, 3765.
[48] B. Zhao, H. Hu, S. K. Mandal, R. C. Haddon, *Chem. Mater.* **2005**, *17*, 3235.
[49] M. Naebe, T. Lin, M. P. Staiger, L. M. Dai, X. G. Wang, *Nanotechnology* **2008**, *19*, 1.

DOI: 10.1002/mame.200900110